The Complete Set of Dyadic Green's Functions for the Parallel-Plate Chirowaveguide and the Application to the Coaxial-Probe Excitation Method

Hon-Tat Hui, *Member, IEEE*, Edward K. N. Yung, *Senior Member, IEEE*, and Xin-Qing Sheng

***Abstract*—In this paper, the complete set of four spatial-domain electromagnetic dyadic Green's functions are rigorously derived for the parallel-plate chirowaveguide. These dyadic Green's functions are presented in the cylindrical coordinates, which are found to facilitate numerical calculations. An electric-field integral equation for the coaxial-probe excitation problem is formulated using the dyadic Green's functions, and the moment-method solution is sought. The probe admittance and current distribution along the probe at different chiral levels are obtained. Results show that a substantially higher admittance level is obtained, but the admittance bandwidth decreases with the chiral parameter. Stopbands at which no net power input into the waveguide are observed. This characteristic is found to have no match in the nonchiral waveguide. The computed current distribution along the probe shows a greater current magnitude than that of the nonchiral waveguide. The validity of the numerical solution is checked with the measured values for the nonchiral case.**

***Index Terms*—Chirowaveguide, dyadic Green's function, excitation method.**

I. Introduction

DYADIC GREEN'S functions are important tools for solving electromagnetic boundary value problems. They are necessary for the moment method in computational electromagnetics. In recent years, much research effort has been devoted to the derivation of the electromagnetic dyadic Green's functions for chiral media, which, unfortunately, has only been successful for some simple cases, e.g., dyadic Green's functions in an unbounded chiral medium have been derived by Bassiri *et al.* [1] and Lindell *et al.* [2], the dyadic Green's function in the presence of a chiral sphere by Engheta and Kowarz [3], the spectral dyadic Green's function formulation for a grounded chiral slab by Toscano and Vegni [4], the spectral-domain dyadic Green's function in layered chiral media by Ali *et al.* [5], and the dyadic Green's function for radially multilayered chiral media by Li *et al.* [6]. All these dyadic Green's functions are either involved with chiral/chiral, chiral/dielectric interfaces, or the chiral/perfect electric conductor (PEC) interface, but with spectral-domain formulations. In [7]–[9], the spatial-domain dyadic Green's functions for the cylindrical and parallel-plate chirowaveguides were first formulated by Hui and Yung, and an alternative formulation for the cylindrical chirowaveguide was more recently seen in [10].

In this paper, we generalize the method developed in [7] to derive the complete set of dyadic Green's functions for the parallel-plate chirowaveguide. This set of dyadic Green's functions can be used simultaneously or independently to find both the electric and/or magnetic fields produced by an arbitrary distribution of electric and/or magnetic current sources. All the dyadic Green's functions are derived in the cylindrical coordinates, which leave the expressions with infinite series rather than infinite *improper* integrals, as in [9]. This reduces the difficulty encountered in the numerical calculations. In Section II, the dyadic Green's functions derived are used to analyze the problem of a coaxial probe inside the waveguide. The coaxial probe is to serve as an excitation method. Although investigations of the coaxial-probe excitation method for the nonchiral parallel-plate waveguide have been well researched [11]–[13], the investigation for the chiral parallel-plate waveguide is researched here for the first time. The coaxial probe will be modeled as a thin wire and the moment method is used to obtain numerical solutions. The presence of thin wire in an unbounded chiral medium has been studied by Jaggard *et al.* [14]. Peculiar characteristics such as the rapid decay in currents and the forbidden zone in radiation patterns were observed. In this paper, the admittance seen by the coaxial line and the current distribution along the coaxial probe will be obtained. The variations of the admittance and current distribution with the levels of chirality, length of the probe, and excitation frequency are all shown. The theoretical admittance for the case with a vanishing chirality is compared with measured values. Our analysis shows that there are significant deviations of the admittance and current distribution from the nonchiral case. For example, stopbands at which the admittance virtually vanishes are observed. These stopbands are found to be located near the cutoff frequencies. The admittance and current distribution are, in most of the cases, substantially larger than the nonchiral case.

II. Formulations for the Electromagnetic Dyadic Green's Functions

The parallel-plate chirowaveguide and the coordinate system are shown in Fig. 1. The constitutive equations to characterize

Manuscript received June 16, 1999.

The authors are with the Department of Electronic Engineering, City University of Hong Kong, Kowloon, Hong Kong.

Publisher Item Identifier S 0018-9480(00)09543-0.

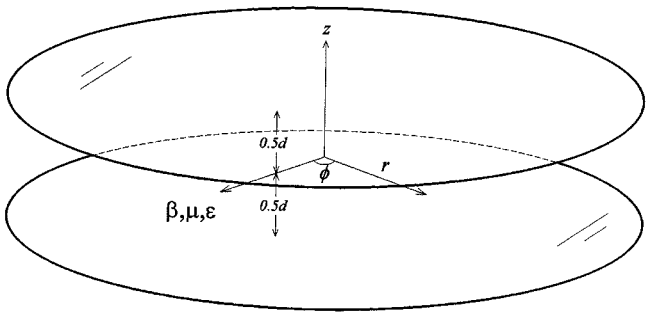

Fig. 1. Parallel-plate chirowaveguide and the coordinate system.

the chiral medium are

$$\vec{D} = \varepsilon\left[\vec{E} + \beta\nabla\times\vec{E}\right] \tag{1a}$$

$$\vec{B} = \mu\left[\vec{H} + \beta\nabla\times\vec{H}\right] \tag{1b}$$

where ε, μ, and β are, respectively, the permittivity, permeability, and chiral parameter of the chiral medium Note that ε, μ, and β are complex numbers in the most general case, but we consider only the lossless case. Equation (1) is the Drude–Born–Fedorov (DBF) form of constitutive equations [15]. For time–harmonic (with the convention $e^{-j\omega t}$) fields and sources, by putting (1) into the Maxwell's equations, we obtain the following vector wave equations for the electric and magnetic fields:

$$\begin{aligned}&\nabla\times\nabla\times\vec{E} - 2\gamma^2\beta\nabla\times\vec{E} - \gamma^2\vec{E}\\ &\quad = j\omega\mu\,(\gamma/k)^2\left[\vec{J} + \beta\nabla\times\vec{J}\right] - (\gamma/k)^2\nabla\times\vec{K}\end{aligned} \tag{2a}$$

$$\begin{aligned}&\nabla\times\nabla\times\vec{H} - 2\gamma^2\beta\nabla\times\vec{H} - \gamma^2\vec{H}\\ &\quad = j\omega\varepsilon\,(\gamma/k)^2\left[\vec{K} + \beta\nabla\times\vec{K}\right] + (\gamma/k)^2\nabla\times\vec{J}\end{aligned} \tag{2b}$$

where $\vec{K}$ and $\vec{J}$ are, respectively, the magnetic and electric current densities and $k = \omega\sqrt{\mu\varepsilon}$, $\gamma^2 = k^2/(1-k^2\beta^2)$. Unique solutions for the electromagnetic field can be obtained by specifying the following boundary condition on the electric field:

$$\hat{n}\times\vec{E}\Big|_{z=\pm 1/2d} = 0 \tag{3}$$

where $\hat{n}$ is a unit normal outward-pointing vector defined on the conducting plates of the waveguide. The right-hand side of (2) implies that we can divide the electric or magnetic field into two parts: one is due to the electric current, denoted by $\vec{E}_J$ and $\vec{H}_J$, and the other is due to the magnetic current, denoted by $\vec{E}_K$ and $\vec{H}_K$. That is, we can separate (2) into the following four equations:

$$\begin{aligned}&\nabla\times\nabla\times\vec{E}_J - 2\gamma^2\beta\nabla\times\vec{E}_J - \gamma^2\vec{E}_J\\ &\quad = j\omega\mu\,(\gamma/k)^2\left[\vec{J} + \beta\nabla\times\vec{J}\right]\end{aligned} \tag{4a}$$

$$\begin{aligned}&\nabla\times\nabla\times\vec{H}_J - 2\gamma^2\beta\nabla\times\vec{H}_J - \gamma^2\vec{H}_J\\ &\quad = (\gamma/k)^2\nabla\times\vec{J}\end{aligned} \tag{4b}$$

$$\begin{aligned}&\nabla\times\nabla\times\vec{E}_K - 2\gamma^2\beta\nabla\times\vec{E}_K - \gamma^2\vec{E}_K\\ &\quad = -(\gamma/k)^2\nabla\times\vec{K}\end{aligned} \tag{4c}$$

$$\begin{aligned}&\nabla\times\nabla\times\vec{H}_K - 2\gamma^2\beta\nabla\times\vec{H}_K - \gamma^2\vec{H}_K\\ &\quad = j\omega\varepsilon\,(\gamma/k)^2\left[\vec{K} + \beta\nabla\times\vec{K}\right].\end{aligned} \tag{4d}$$

Note that since the electric and magnetic currents are, in general, independent of each other, the *partial* electric fields in (4a) and (4c) must satisfy the same boundary conditions as (3), namely,

$$\hat{n}\times\vec{E}_J\Big|_{z=\pm 1/2d} = \hat{n}\times\vec{E}_K\Big|_{z=\pm 1/2d} = 0. \tag{5}$$

The total electric and magnetic fields $\vec{E}$ and $\vec{H}$ will be the sum of the partial fields in (4a)–(4d).

We notice from (4b) and (4c) that $\nabla\cdot\vec{H}_J = 0$ and $\nabla\cdot\vec{E}_K = 0$. This is an important consequence of the partial-field expression, and this gives us a great convenience in deriving the dyadic Green's functions because the fact that these two partial fields are divergenceless allows us to expand them completely by using only the solenoidal vector wave functions. In view of (4), the equations for the dyadic Green's functions and boundary conditions can be written as

$$\begin{aligned}&\nabla\times\nabla\times\overline{\overline{G}}_{EJ}\left(\vec{R},\vec{R}'\right) - 2\gamma^2\beta\nabla\times\overline{\overline{G}}_{EJ}\left(\vec{R},\vec{R}'\right)\\ &\qquad - \gamma^2\overline{\overline{G}}_{EJ}\left(\vec{R},\vec{R}'\right)\\ &\quad = (\gamma/k)^2\left\{\overline{\overline{I}}\delta\left(\vec{R}-\vec{R}'\right) + \beta\nabla\times\left[\overline{\overline{I}}\delta\left(\vec{R}-\vec{R}'\right)\right]\right\}\end{aligned} \tag{6a}$$

$$\begin{aligned}&\nabla\times\nabla\times\overline{\overline{G}}_{HJ}\left(\vec{R},\vec{R}'\right) - 2\gamma^2\beta\nabla\times\overline{\overline{G}}_{HJ}\left(\vec{R},\vec{R}'\right)\\ &\qquad - \gamma^2\overline{\overline{G}}_{HJ}\left(\vec{R},\vec{R}'\right)\\ &\quad = (\gamma/k)^2\nabla\times\left[\overline{\overline{I}}\delta\left(\vec{R}-\vec{R}'\right)\right]\end{aligned} \tag{6b}$$

$$\begin{aligned}&\nabla\times\nabla\times\overline{\overline{G}}_{EK}\left(\vec{R},\vec{R}'\right) - 2\gamma^2\beta\nabla\times\overline{\overline{G}}_{EK}\left(\vec{R},\vec{R}'\right)\\ &\qquad - \gamma^2\overline{\overline{G}}_{EK}\left(\vec{R},\vec{R}'\right)\\ &\quad = -(\gamma/k)^2\nabla\times\left[\overline{\overline{I}}\delta\left(\vec{R}-\vec{R}'\right)\right]\end{aligned} \tag{6c}$$

$$\begin{aligned}&\nabla\times\nabla\times\overline{\overline{G}}_{HK}\left(\vec{R},\vec{R}'\right) - 2\gamma^2\beta\nabla\times\overline{\overline{G}}_{HK}\left(\vec{R},\vec{R}'\right)\\ &\qquad - \gamma^2\overline{\overline{G}}_{HK}\left(\vec{R},\vec{R}'\right)\\ &\quad = (\gamma/k)^2\left\{\overline{\overline{I}}\delta\left(\vec{R}-\vec{R}'\right) + \beta\nabla\times\left[\overline{\overline{I}}\delta\left(\vec{R}-\vec{R}'\right)\right]\right\}\end{aligned} \tag{6d}$$

$$\begin{aligned}&\hat{n}\times\overline{\overline{G}}_{EJ}\left(\vec{R},\vec{R}'\right)\Big|_{z=\pm 1/2d}\\ &\quad = \hat{n}\times\overline{\overline{G}}_{EK}\left(\vec{R},\vec{R}'\right)\Big|_{z=\pm 1/2d}\\ &\quad = 0\end{aligned} \tag{7}$$

where $\overline{\overline{I}}$ is the unit dyadic, $\delta(\vec{R}-\vec{R}')$ is the three-dimensional delta function, $\vec{R}$ is the field coordinate point, and $\vec{R}'$ is the source coordinate point. Note that although $\overline{\overline{G}}_{EJ}(\vec{R},\vec{R}')$ and $\overline{\overline{G}}_{HK}(\vec{R},\vec{R}')$ are governed by the same equation, the boundary conditions for them are different. Therefore, solutions to them must be different. The same inference also applies to $\overline{\overline{G}}_{HJ}(\vec{R},\vec{R}')$ and $\overline{\overline{G}}_{EK}(\vec{R},\vec{R}')$. Furthermore, the four dyadic Green's functions in (6) are not all independent. They are

connected by the following relations:

$$\overline{\overline{G}}_{EJ}\left(\vec{R},\vec{R}'\right)=\frac{1}{\gamma^2}\nabla\times\overline{\overline{G}}_{HJ}\left(\vec{R},\vec{R}'\right)-\beta\overline{\overline{G}}_{HJ}\left(\vec{R},\vec{R}'\right)-\frac{1}{k^2}\overline{\overline{I}}\delta\left(\vec{R}-\vec{R}'\right) \tag{8a}$$

$$\overline{\overline{G}}_{HK}\left(\vec{R},\vec{R}'\right)=\frac{1}{\gamma^2}\nabla\times\overline{\overline{G}}_{EK}\left(\vec{R},\vec{R}'\right)-\beta\overline{\overline{G}}_{EK}\left(\vec{R},\vec{R}'\right)-\frac{1}{k^2}\overline{\overline{I}}\delta\left(\vec{R}-\vec{R}'\right). \tag{8b}$$

These two relations can be obtained by considering similar relations between the electric and magnetic fields.

By using the linearity property of the operators $\nabla\times\nabla\times$ and $\nabla\times$, and right-multiplying an elementary current source to (6a)–(6d) and integrating, we can establish the integral relations between the dyadic Green's functions and the field quantities, i.e.,

$$\vec{E}\left(\vec{R}\right)=j\omega\mu\iiint_v\overline{\overline{G}}_{EJ}\left(\vec{R},\vec{R}'\right)\cdot\vec{J}\left(\vec{R}'\right)dv'-\iiint_v\overline{\overline{G}}_{EK}\left(\vec{R},\vec{R}'\right)\cdot\vec{K}\left(\vec{R}'\right)dv' \tag{9a}$$

$$\vec{H}\left(\vec{R}\right)=\iiint_v\overline{\overline{G}}_{HJ}\left(\vec{R},\vec{R}'\right)\cdot\vec{J}\left(\vec{R}'\right)dv'+j\omega\varepsilon\iiint_v\overline{\overline{G}}_{HK}\left(\vec{R},\vec{R}'\right)\cdot\vec{K}\left(\vec{R}'\right)dv' \tag{9b}$$

where v is the volume containing the current sources. From (9a) and (9b), $\overline{\overline{G}}_{EJ}(\vec{R},\vec{R}')$ is identified as the electric dyadic Green's function for an electric current source, $\overline{\overline{G}}_{EK}(\vec{R},\vec{R}')$ as the electric dyadic Green's function for a magnetic current source, $\overline{\overline{G}}_{HJ}(\vec{R},\vec{R}')$ as the magnetic dyadic Green's function for an electric current source, and $\overline{\overline{G}}_{HK}(\vec{R},\vec{R}')$ as the magnetic dyadic Green's function for a magnetic current source. These dyadic Green's functions are of great importance to solving waveguide problems. It is obvious from (9) that none of these dyadic Green's functions alone can yield a complete solution to the electric or magnetic fields.

To find these dyadic Green's functions, we use the similar technique as in [9] or [7] and [8]. We first seek expressions of the electric and magnetic fields in a source-free region expanded in terms of their eigenfunctions. This can be done by transforming the electric and magnetic fields into two fields $\vec{Q}_1$ and $\vec{Q}_2$, which satisfy the nonchiral isotropic vector wave equation. The transformed fields $\vec{Q}_1$ and $\vec{Q}_2$ are divergenceless and, hence, can be expanded by the solenoidal vector wave functions. In this way, the eigenfunctions of the electric and magnetic fields can be expressed as linear combinations of the $\vec{M}$ and $\vec{N}$ vector wave functions. The complete eigenfunction expansions of the electric and magnetic fields can then be obtained by further determining the expansion coefficients. It is from the expansion of the magnetic field that we finally recover the expression of the magnetic dyadic Green's function. This is possible because of the condition that the expansion of the purely solenoidal magnetic field is complete. In the present case, since we have expressed the electric and magnetic fields as *partial* fields, we have two purely solenoidal fields $\vec{H}_J$ and $\vec{E}_K$, i.e., the magnetic field due to an electric current and the electric field due to a magnetic current. Thus, by the same token, we can derive $\overline{\overline{G}}_{EK}(\vec{R},\vec{R}')$ and $\overline{\overline{G}}_{HJ}(\vec{R},\vec{R}')$. Without going into the detailed steps (which are similar to those laid out in [9]), we just spell out the final results of the derivation shown in (10) and (11), at the bottom of the following page, where

$$\vec{E}^{+}_{\substack{\varepsilon\\o}en}(\lambda_e,k_{z1e},k_{z2e})=\cos(k_{z2e}1/2\,d)\vec{Q}^{(1)}_{1\substack{\varepsilon\\o}en}(\lambda_e,k_{z1e})-\cos(k_{z1e}1/2\,d)\vec{Q}^{(1)}_{2\substack{\varepsilon\\o}en}(\lambda_e,k_{z2e}) \tag{12a}$$

$$\vec{E}^{+}_{\substack{\varepsilon\\o}on}(\lambda_o,k_{z1o},k_{z2o})=\sin(k_{z2o}1/2\,d)\vec{Q}^{(1)}_{1\substack{\varepsilon\\o}on}(\lambda_o,k_{z1o})-\sin(k_{z1o}1/2\,d)\vec{Q}^{(1)}_{2\substack{\varepsilon\\o}on}(\lambda_o,k_{z2o}) \tag{12b}$$

$$\vec{E}^{-}_{\substack{\varepsilon\\o}en}(\lambda_e,k_{z1e},k_{z2e})=\cos(k_{z2e}1/2\,d)\vec{Q}_{1\substack{\varepsilon\\o}en}(\lambda_e,k_{z1e})-\cos(k_{z1e}1/2\,d)\vec{Q}_{2\substack{\varepsilon\\o}en}(\lambda_e,k_{z2e}) \tag{12c}$$

$$\vec{E}^{-}_{\substack{\varepsilon\\o}on}(\lambda_o,k_{z1o},k_{z2o})=\sin(k_{z2o}1/2\,d)\vec{Q}_{1\substack{\varepsilon\\o}on}(\lambda_o,k_{z1o})-\sin(k_{z1o}1/2\,d)\vec{Q}_{2\substack{\varepsilon\\o}on}(\lambda_o,k_{z2o}) \tag{12d}$$

$$\vec{H}^{+}_{\substack{\varepsilon\\o}en}(\lambda_e,k_{z1e},k_{z2e})=\frac{k}{j\omega\mu}\left[\cos(k_{z2e}1/2\,d)\vec{Q}^{(1)}_{1\substack{\varepsilon\\o}en}(\lambda_e,k_{z1e})+\cos(k_{z1e}1/2\,d)\vec{Q}^{(1)}_{2\substack{\varepsilon\\o}en}(\lambda_e,k_{z2e})\right] \tag{12e}$$

$$\vec{H}^{+}_{\substack{\varepsilon\\o}on}(\lambda_o,k_{z1o},k_{z2o})=\frac{k}{j\omega\mu}\left[\sin(k_{z2o}1/2\,d)\vec{Q}^{(1)}_{1\substack{\varepsilon\\o}on}(\lambda_o,k_{z1o})+\sin(k_{z1o}1/2\,d)\vec{Q}^{(1)}_{2\substack{\varepsilon\\o}on}(\lambda_o,k_{z2o})\right] \tag{12f}$$

$$\vec{H}^{-}_{\substack{\varepsilon\\o}en}(\lambda_e,k_{z1e},k_{z2e})=\frac{k}{j\omega\mu}\left[\cos(k_{z2e}1/2\,d)\vec{Q}_{1\substack{\varepsilon\\o}en}(\lambda_e,k_{z1e})+\cos(k_{z1e}1/2\,d)\vec{Q}_{2\substack{\varepsilon\\o}en}(\lambda_e,k_{z2e})\right] \tag{12g}$$

$$\vec{H}^{-}_{\substack{\varepsilon\\o}on}(\lambda_o,k_{z1o},k_{z2o})=\frac{k}{j\omega\mu}\left[\sin(k_{z2o}1/2\,d)\vec{Q}_{1\substack{\varepsilon\\o}on}(\lambda_o,k_{z1o})+\sin(k_{z1o}1/2\,d)\vec{Q}_{2\substack{\varepsilon\\o}on}(\lambda_o,k_{z2o})\right] \tag{12h}$$

$$I_e=\frac{2k}{\omega\mu}(1+\delta_{n0})\lambda_e^2\cdot\left\{\frac{\cos^2(k_{z2e}1/2\,d)}{k_1}\left[d+\frac{\sin(k_{z1e}d)}{k_{z1e}}\right]+\frac{\cos^2(k_{z1e}1/2\,d)}{k_2}\left[d+\frac{\sin(k_{z2e}d)}{k_{z2e}}\right]\right\} \tag{13a}$$

$$I_o=\frac{2k}{\omega\mu}(1+\delta_{n0})\lambda_o^2\left\{\frac{\sin^2(k_{z2o}1/2\,d)}{k_1}\left[d-\frac{\sin(k_{z1o}d)}{k_{z1o}}\right]+\frac{\sin^2(k_{z1o}1/2\,d)}{k_2}\left[d-\frac{\sin(k_{z2o}d)}{k_{z2o}}\right]\right\} \tag{13b}$$

and δ_{n0} is the Kronecker delta defined with respect to n. The transformed fields are expanded in terms of the vector wave functions as

$$\vec{Q}_{1\substack{\varepsilon_e\\ \varepsilon_o}en}(\lambda_e, k_{z1e}) = \vec{M}_{\substack{\varepsilon_e\\ \varepsilon_o}en}(\lambda_e, k_{z1e}) + \vec{N}_{\substack{\varepsilon_e\\ \varepsilon_o}en}(\lambda_e, k_{z1e}) \tag{14a}$$

$$\vec{Q}_{1\substack{\varepsilon_e\\ \varepsilon_o}on}(\lambda_o, k_{z1o}) = \vec{M}_{\substack{\varepsilon_e\\ \varepsilon_o}on}(\lambda_o, k_{z1o}) + \vec{N}_{\substack{\varepsilon_e\\ \varepsilon_o}on}(\lambda_o, k_{z1o}) \tag{14b}$$

$$\vec{Q}_{2\substack{\varepsilon_e\\ \varepsilon_o}en}(\lambda_e, k_{z2e}) = \vec{M}_{\substack{\varepsilon_e\\ \varepsilon_o}en}(\lambda_e, k_{z2e}) - \vec{N}_{\substack{\varepsilon_e\\ \varepsilon_o}en}(\lambda_e, k_{z2e}) \tag{14c}$$

$$\vec{Q}_{2\substack{\varepsilon_e\\ \varepsilon_o}on}(\lambda_o, k_{z2o}) = \vec{M}_{\substack{\varepsilon_e\\ \varepsilon_o}on}(\lambda_o, k_{z2o}) - \vec{N}_{\substack{\varepsilon_e\\ \varepsilon_o}on}(\lambda_o, k_{z2o}) \tag{14d}$$

where

$$\vec{M}_{\substack{\varepsilon_e\\ \varepsilon_o}en}(\lambda_e, k_{zie}) = \mp \frac{nJ_n(\lambda_e r)}{r} \begin{matrix}\sin\\ \cos\end{matrix} n\phi \cos(k_{zie}z)\hat{r} - \frac{\partial J_n(\lambda_e r)}{\partial r} \begin{matrix}\cos\\ \sin\end{matrix} n\phi \cos(k_{zie}z)\hat{\phi} \tag{15a}$$

$$\vec{N}_{\substack{\varepsilon_e\\ \varepsilon_o}en}(\lambda_e, k_{zie}) = \frac{1}{k_i}\left[-k_{zie}\frac{\partial J_n(\lambda_e r)}{\partial r} \begin{matrix}\cos\\ \sin\end{matrix} n\phi \sin(k_{zie}z)\hat{r} \pm k_{zie}\frac{nJ_n(\lambda_e r)}{r} \begin{matrix}\sin\\ \cos\end{matrix} n\phi \sin(k_{zie}z)\hat{\phi} + \lambda_e^2 J_n(\lambda_e r) \begin{matrix}\cos\\ \sin\end{matrix} n\phi \cos(k_{zie}z)\hat{z}\right] \tag{15b}$$

$$\vec{M}_{\substack{\varepsilon_e\\ \varepsilon_o}on}(\lambda_o, k_{zio}) = \mp \frac{nJ_n(\lambda_o r)}{r} \begin{matrix}\sin\\ \cos\end{matrix} n\phi \sin(k_{zio}z)\hat{r} - \frac{\partial J_n(\lambda_o r)}{\partial r} \begin{matrix}\cos\\ \sin\end{matrix} n\phi \sin(k_{zio}z)\hat{\phi} \tag{15c}$$

$$\vec{N}_{\substack{\varepsilon_e\\ \varepsilon_o}on}(\lambda_o, k_{zio}) = \frac{1}{k_i}\left[k_{zio}\frac{\partial J_n(\lambda_o r)}{\partial r} \begin{matrix}\cos\\ \sin\end{matrix} n\phi \cos(k_{zio}z)\hat{r} \mp k_{zio}\frac{nJ_n(\lambda_o r)}{r} \begin{matrix}\sin\\ \cos\end{matrix} n\phi \cos(k_{zio}z)\hat{\phi} + \lambda_o^2 J_n(\lambda_o r) \begin{matrix}\cos\\ \sin\end{matrix} n\phi \sin(k_{zio}z)\hat{z}\right] \tag{15d}$$

and

$$\lambda_e^2 + k_{zie}^2 = k_i^2 \tag{16a}$$

$$\lambda_o^2 + k_{zio}^2 = k_i^2, \qquad i = 1, 2. \tag{16b}$$

In (15), J_n is the Bessel function of the first kind and order n. The propagation constants in (16) are given by [9]

$$k_1 = \frac{k}{1 - k\beta} \tag{17a}$$

$$k_2 = \frac{k}{1 + k\beta}. \tag{17b}$$

In the expressions of $\overline{\overline{G}}_{HJ}(\vec{R}, \vec{R}')$ $\overline{\overline{G}}_{EK}(\vec{R}, \vec{R}')$, the primed eigenfunctions are defined with respect to the source coordinates r', ϕ', z'. The superscript "(1)" in (12) is to indicate that the Bessel function in the transformed fields are replaced with

---

$$\overline{\overline{G}}^{\pm}_{HJ}(\vec{R}, \vec{R}') = \sum_m \sum_n (\gamma/k)^2 \begin{cases} \left\{\frac{1}{I_e}\vec{H}^{+}_{\substack{\varepsilon_e\\ \varepsilon_o}en}(\lambda_e, k_{z1e}, k_{z2e})\left[-\vec{E}'^{-}_{\substack{\varepsilon_e\\ \varepsilon_o}en}(\lambda_e, k_{z1e}, k_{z2e}) - j\omega\mu\beta\vec{H}'^{-}_{\substack{\varepsilon_e\\ \varepsilon_o}en}(\lambda_e, k_{z1e}, k_{z2e})\right]\right. \\ \left. + \frac{1}{I_o}\vec{H}^{+}_{\substack{\varepsilon_e\\ \varepsilon_o}on}(\lambda_o, k_{z1o}, k_{z2o})\left[-\vec{E}'^{-}_{\substack{\varepsilon_e\\ \varepsilon_o}on}(\lambda_o, k_{z1o}, k_{z2o}) - j\omega\mu\beta\vec{H}'^{-}_{\substack{\varepsilon_e\\ \varepsilon_o}on}(\lambda_o, k_{z1o}, k_{z2o})\right]\right\}, & r > r' \\ \left\{\frac{1}{I_e}\vec{H}^{-}_{\substack{\varepsilon_e\\ \varepsilon_o}en}(\lambda_e, k_{z1e}, k_{z2e})\left[-\vec{E}'^{+}_{\substack{\varepsilon_e\\ \varepsilon_o}en}(\lambda_e, k_{z1e}, k_{z2e}) - j\omega\mu\beta\vec{H}'^{+}_{\substack{\varepsilon_e\\ \varepsilon_o}en}(\lambda_e, k_{z1e}, k_{z2e})\right]\right. \\ \left. + \frac{1}{I_o}\vec{H}^{-}_{\substack{\varepsilon_e\\ \varepsilon_o}on}(\lambda_o, k_{z1o}, k_{z2o})\left[-\vec{E}'^{+}_{\substack{\varepsilon_e\\ \varepsilon_o}on}(\lambda_o, k_{z1o}, k_{z2o}) - j\omega\mu\beta\vec{H}'^{+}_{\substack{\varepsilon_e\\ \varepsilon_o}on}(\lambda_o, k_{z1o}, k_{z2o})\right]\right\}, & r < r' \end{cases} \tag{10}$$

$$\overline{\overline{G}}^{\pm}_{EK}(\vec{R}, \vec{R}') = -\sum_m \sum_n (\gamma/k)^2 \begin{cases} \left\{\frac{1}{I_e}\vec{E}^{+}_{\substack{\varepsilon_e\\ \varepsilon_o}en}(\lambda_e, k_{z1e}, k_{z2e})[-j\omega\varepsilon\beta\vec{E}'^{-}_{\substack{\varepsilon_e\\ \varepsilon_o}en}(\lambda_e, k_{z1e}, k_{z2e}) + \vec{H}'^{-}_{\substack{\varepsilon_e\\ \varepsilon_o}en}(\lambda_e, k_{z1e}, k_{z2e})]\right. \\ \left. + \frac{1}{I_o}\vec{E}^{+}_{\substack{\varepsilon_e\\ \varepsilon_o}on}(\lambda_o, k_{z1o}, k_{z2o})[-j\omega\varepsilon\beta\vec{E}'^{-}_{\substack{\varepsilon_e\\ \varepsilon_o}on}(\lambda_o, k_{z1o}, k_{z2o}) + \vec{H}'^{-}_{\substack{\varepsilon_e\\ \varepsilon_o}on}(\lambda_o, k_{z1o}, k_{z2o})]\right\}, & r > r' \\ \left\{\frac{1}{I_e}\vec{E}^{-}_{\substack{\varepsilon_e\\ \varepsilon_o}en}(\lambda_e, k_{z1e}, k_{z2e})[-j\omega\varepsilon\beta\vec{E}'^{+}_{\substack{\varepsilon_e\\ \varepsilon_o}en}(\lambda_e, k_{z1e}, k_{z2e}) + \vec{H}'^{+}_{\substack{\varepsilon_e\\ \varepsilon_o}en}(\lambda_e, k_{z1e}, k_{z2e})]\right. \\ \left. + \frac{1}{I_o}\vec{E}^{-}_{\substack{\varepsilon_e\\ \varepsilon_o}on}(\lambda_o, k_{z1o}, k_{z2o})[-j\omega\varepsilon\beta\vec{E}'^{+}_{\substack{\varepsilon_e\\ \varepsilon_o}on}(\lambda_o, k_{z1o}, k_{z2o}) + \vec{H}'^{+}_{\substack{\varepsilon_e\\ \varepsilon_o}on}(\lambda_o, k_{z1o}, k_{z2o})]\right\}, & r < r' \end{cases} \tag{11}$$

the Hankel function of the first kind. This is for the case for expressing the fields for $r > r'$. The index m in the double summation counts over all the roots of the dispersion equations, i.e., λ_e and λ_o. The relations of $\overline{\overline{G}}^{\pm}_{HJ}(\vec{R}, \vec{R}')$ to $\overline{\overline{G}}_{HJ}(\vec{R}, \vec{R}')$ and $\overline{\overline{G}}^{\pm}_{EK}(\vec{R}, \vec{R}')$ to $\overline{\overline{G}}_{EK}(\vec{R}, \vec{R}')$ are [16]

$$\overline{\overline{G}}_{HJ}(\vec{R}, \vec{R}') = \overline{\overline{G}}^{+}_{HJ}(\vec{R}, \vec{R}')U(r - r') + \overline{\overline{G}}^{-}_{HJ}(\vec{R}, \vec{R}')U(r' - r) \tag{18}$$

$$\overline{\overline{G}}_{EK}(\vec{R}, \vec{R}') = \overline{\overline{G}}^{+}_{EK}(\vec{R}, \vec{R}')U(r - r') + \overline{\overline{G}}^{-}_{EK}(\vec{R}, \vec{R}')U(r' - r) \tag{19}$$

where $U(r-r')$ and $U(r'-r)$ are two unit step functions defined as in [16, pp. 107] With $\overline{\overline{G}}_{HJ}(\vec{R}, \vec{R}')$ and $\overline{\overline{G}}_{EK}(\vec{R}, \vec{R}')$, the remaining two dyadic Green's functions can be found from the relations in (8a) and (8b). They are shown in (20) and (21) at the bottom of this page. Thus, all the four dyadic Green's functions in (6a) and (6b) have been obtained. In the following section, we shall apply two of these dyadic Green's functions to analyze the problem of the coaxial-probe excitation for the waveguide.

III. Application to the Coaxial-Probe Excitation

Consider the parallel-plate chirowaveguide excited by a coaxial probe, as shown in Fig. 2. The chiral medium filling the waveguide is assumed to be lossless and $\mu = \mu_0$, $\varepsilon = \varepsilon_0$. The coaxial probe has a length ℓ and radius a. The radius of the outer conductor of the coaxial line is b. A thin probe (with

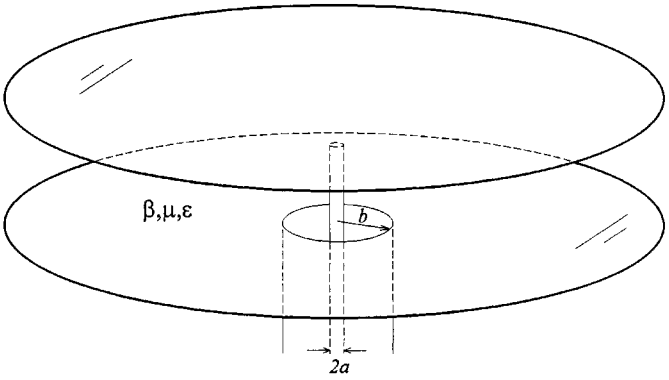

Fig. 2. Coaxial-feed excitation method of the parallel-plate chirowaveguide.

$a \ll \lambda$ where λ is the excitation wavelength), as commonly used for the excitation of the nonchiral parallel-plate waveguide, is considered in this paper. This allows us to use the thin-wire approximation in the following analysis. We can identify two current sources in this problem: the electric current $\vec{I}$ on the coaxial probe and the magnetic current $\vec{K}$ over the coaxial aperture. A TEM mode distribution for $\vec{K}$ is assumed as follows:

$$\vec{K} = \frac{V_{ab}}{r \log(b/a)}\,\hat{\phi} \tag{22}$$

where V_{ab} is the voltage applied across the inner and outer conductors of the coaxial line.

$$\begin{aligned}
&\overline{\overline{G}}_{EJ}(\vec{R}, \vec{R}') \\
&\quad = -\frac{1}{k^2}\hat{r}\hat{r}\delta(\vec{R} - \vec{R}') + \frac{1}{j\omega\mu}\sum_m\sum_n(\gamma/k)^2 \\
&\qquad \cdot \begin{cases}
\left\{\frac{1}{I_e}\vec{E}^{+}_{\substack{e\\o}en}(\lambda_e, k_{z1e}, k_{z2e})\left[-\vec{E}'^{-}_{\substack{e\\o}en}(\lambda_e, k_{z1e}, k_{z2e}) - j\omega\mu\beta\vec{H}'^{-}_{\substack{e\\o}en}(\lambda_e, k_{z1e}, k_{z2e})\right]\right. \\
\quad \left. + \frac{1}{I_o}\vec{E}^{+}_{\substack{e\\o}on}(\lambda_o, k_{z1o}, k_{z2o})\left[-\vec{E}'^{-}_{\substack{e\\o}on}(\lambda_o, k_{z1o}, k_{z2o}) - j\omega\mu\beta\vec{H}'^{-}_{\substack{e\\o}on}(\lambda_o, k_{z1o}, k_{z2o})\right]\right\}, & r > r' \\
\left\{\frac{1}{I_e}\vec{E}^{-}_{\substack{e\\o}en}(\lambda_e, k_{z1e}, k_{z2e})\left[-\vec{E}'^{+}_{\substack{e\\o}en}(\lambda_e, k_{z1e}, k_{z2e}) - j\omega\mu\beta\vec{H}'^{+}_{\substack{e\\o}en}(\lambda_e, k_{z1e}, k_{z2e})\right]\right. \\
\quad \left. + \frac{1}{I_o}\vec{E}^{-}_{\substack{e\\o}on}(\lambda_o, k_{z1o}, k_{z2o})\left[-\vec{E}'^{+}_{\substack{e\\o}on}(\lambda_o, k_{z1o}, k_{z2o}) - j\omega\mu\beta\vec{H}'^{+}_{\substack{e\\o}on}(\lambda_o, k_{z1o}, k_{z2o})\right]\right\}, & r < r'
\end{cases}
\end{aligned} \tag{20}$$

$$\begin{aligned}
&\overline{\overline{G}}_{HK}(\vec{R}, \vec{R}') \\
&\quad = -\frac{1}{k^2}\hat{r}\hat{r}\delta(\vec{R} - \vec{R}') + \frac{1}{j\omega\varepsilon}\sum_m\sum_n(\gamma/k)^2 \\
&\qquad \cdot \begin{cases}
\left\{\frac{1}{I_e}\vec{H}^{+}_{\substack{e\\o}en}(\lambda_e, k_{z1e}, k_{z2e})\left[-j\omega\varepsilon\beta\vec{E}'^{-}_{\substack{e\\o}en}(\lambda_e, k_{z1e}, k_{z2e}) + \vec{H}'^{-}_{\substack{e\\o}en}(\lambda_e, k_{z1e}, k_{z2e})\right]\right. \\
\quad \left. + \frac{1}{I_o}\vec{H}^{+}_{\substack{e\\o}on}(\lambda_o, k_{z1o}, k_{z2o})\left[-j\omega\varepsilon\beta\vec{E}'^{-}_{\substack{e\\o}on}(\lambda_o, k_{z1o}, k_{z2o}) + \vec{H}'^{-}_{\substack{e\\o}on}(\lambda_o, k_{z1o}, k_{z2o})\right]\right\}, & r > r' \\
\left\{\frac{1}{I_e}\vec{H}_{\substack{e\\o}en}{}^{-}(\lambda_e, k_{z1e}, k_{z2e})\left[-j\omega\varepsilon\beta\vec{E}'^{+}_{\substack{e\\o}en}(\lambda_e, k_{z1e}, k_{z2e}) + \vec{H}'^{+}_{\substack{e\\o}en}(\lambda_e, k_{z1e}, k_{z2e})\right]\right. \\
\quad \left. + \frac{1}{I_o}\vec{H}^{-}_{\substack{e\\o}on}(\lambda_o, k_{z1o}, k_{z2o})\left[-j\omega\varepsilon\beta\vec{E}'^{+}_{\substack{e\\o}on}(\lambda_o, k_{z1o}, k_{z2o}) + \vec{H}'^{+}_{\substack{e\\o}on}(\lambda_o, k_{z1o}, k_{z2o})\right]\right\}, & r < r'
\end{cases}
\end{aligned} \tag{21}$$

TABLE I
CONVERGENCE OF THE PROBE ADMITTANCE WITH RESPECT TO m, THE NUMBER OF ROOTS OF THE DISPERSION EQUATIONS ($d = 1$ cm, $a = 0.015$ cm, $b = 2.25a$, $\ell = d$, $ka = 0.0664$, $kd = 4.42$)

m	Admittance (mS) for β = 0.0003m	Admittance (mS) for β = 0.0007m	Admittance (mS) for $\beta = 0$
46	3.439-j0.780	1.918+j22.791	2.461+j1.973
62	3.437-j0.766	1.917+j22.807	2.461+j1.986
78	3.437-j0.755	1.917+j22.821	2.461+j1.996
95	3.437-j0.736	1.917+j22.842	2.461+j2.015
100	3.437-j0.733	1.917+j22.846	2.461+j2.019

By using the electric dyadic Green's function for an electric current source $\overline{\overline{G}}_{EJ}(\vec{R}, \vec{R}')$ and the electric dyadic Green's function for a magnetic current source $\overline{\overline{G}}_{EK}(\vec{R}, \vec{R}')$, an electric-field integral equation (EFIE) on the surface of the probe can be formulated

$$\int_0^{\ell} \left[\overline{\overline{G}}_{EJ}(r,\phi,z;r',\phi',z')\right]_{\hat{z}\hat{z}} \cdot \vec{I}(z')\,dz' - \int_0^{2\pi}\int_a^b \left[\overline{\overline{G}}_{EK}(r,\phi,z;\,r',\phi',z')\right]_{\hat{z}\hat{\phi}} \cdot \vec{K}(r')r'\,dr'\,d\phi' = 0 \tag{23}$$

where $[\overline{\overline{G}}_{EJ}(r, \phi, z;r', \phi', z')]_{\hat{z}\hat{z}}$ is the $\hat{z}\hat{z}$ component of $\overline{\overline{G}}_{EJ}(\vec{R}, \vec{R}')$ and $[\overline{\overline{G}}_{EK}(r, \phi, z;r', \phi', z')]_{\hat{z}\hat{\phi}}$ is the $\hat{z}\hat{\phi}$ component of $\overline{\overline{G}}_{EK}(\vec{R}, \vec{R}')$. We need these two components because the electric current on the probe runs only in the z-direction, while the magnetic current over the coaxial aperture has only the ϕ-direction. The expressions of these two dyadic components and some computation techniques are presented in the Appendix.

IV. NUMERICAL RESULTS AND DISCUSSION

The current along the probe $\vec{I}(z')$ is expanded by the piecewise sinusoidal function and the integral equation in (23) is matched using the Galerkin method. As explained in the Appendix, all the integrations and the infinite series with respect to n can be carried out in closed forms, leaving only the infinite series with respect to m. The convergence of the probe input admittance with respect to m, i.e., the number of roots of the dispersion equations, is shown in Table I. We see that, for both cases of $\beta = 0.0003$ m and $\beta = 0.0007$ m, the difference of the imaginary part of the admittance obtained at $m = 95$ and $m = 100$ has been less than 0.5% and that for the nonchiral case is about 0.2%. Hence, we take $m = 95$ in our subsequent calculations.

In Fig. 3, we compare the probe admittance of two weak chiral cases with the nonchiral one for $ka = 0.0664$, $b = 2.25a$, $d = 1$ cm, and $\ell = d$. We see from this figure that the nonchiral admittance (with $\beta = 0$) agrees quite well with the measurement values obtained by Rao [11]. The chiral admittance of the two weak chiral cases approaches that of the nonchiral one asymptotically. The difference between the chiral admittance at $\beta = 0.00001$ m and the nonchiral admittance is very small in the range of kd values shown in this figure. Note that the chiral parallel-plate waveguide always lacks a TEM mode [17] and, thus, the same observation may not be generalized to all ranges of kd values. Nevertheless, the results in Fig. 3 confirm the validity of our method.

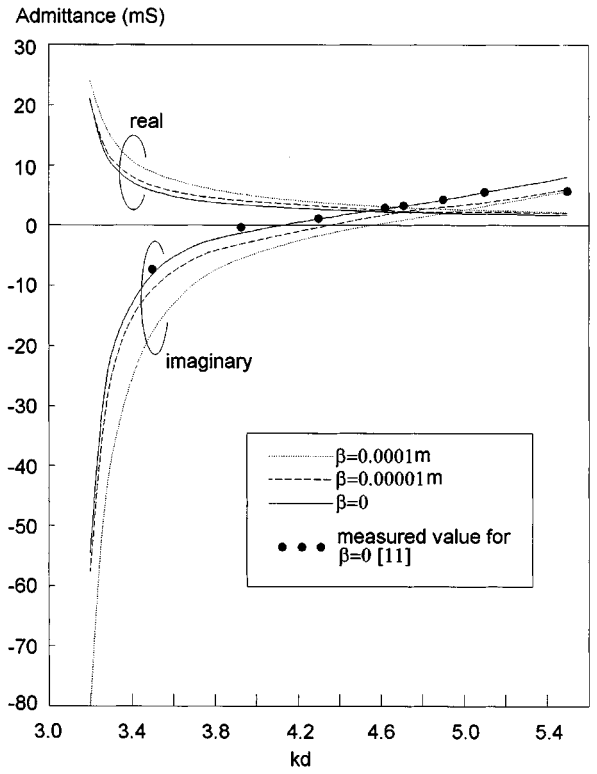

Fig. 3. Comparison of the probe admittances of two weak chiral cases with the nonchiral one.

The variations of the probe admittance with the excitation frequency are shown in Fig. 4(a)–(c) for three different chiral parameters of $\beta = 0.0003$ m, $\beta = 0.0005$ m, and $\beta = 0.0007$ m. The geometric parameters are $d = 1$ cm, $a = 0.01$ cm, $b = 20a$, and $\ell = d$. The case for $\beta = 0$ is also plotted in Fig. 4(a) for comparison. The following observations are obtained from Fig. 4.

1) The chiral admittance (both real and imaginary parts) is generally greater than that of the nonchiral case and increases with the chiral parameter.
2) A greater chiral parameter causes more rapid variations of the admittance, i.e., more ripples can be seen in the same frequency range.
3) There are two frequencies, i.e., 27 GHz in Fig. 4(b) and 25.1 GHz in Fig. 4(c), at which the admittance vanishes. That means the coaxial probe is actually equivalent to an open circuit at these two frequencies. For frequencies close to these two frequencies, the waveguide becomes a very large capacitive or reactive load. That means no net power can be transmitted into waveguide in these frequency bands, which may be termed the *stopbands*. Furthermore, we see from Fig. 4(b) and (c) that a greater chiral parameter gives a wider *stopband*. This is a new phenomenon, which does not find a match for the nonchiral case. We find that these stopbands are located very near the second-lowest cutoff frequencies of the

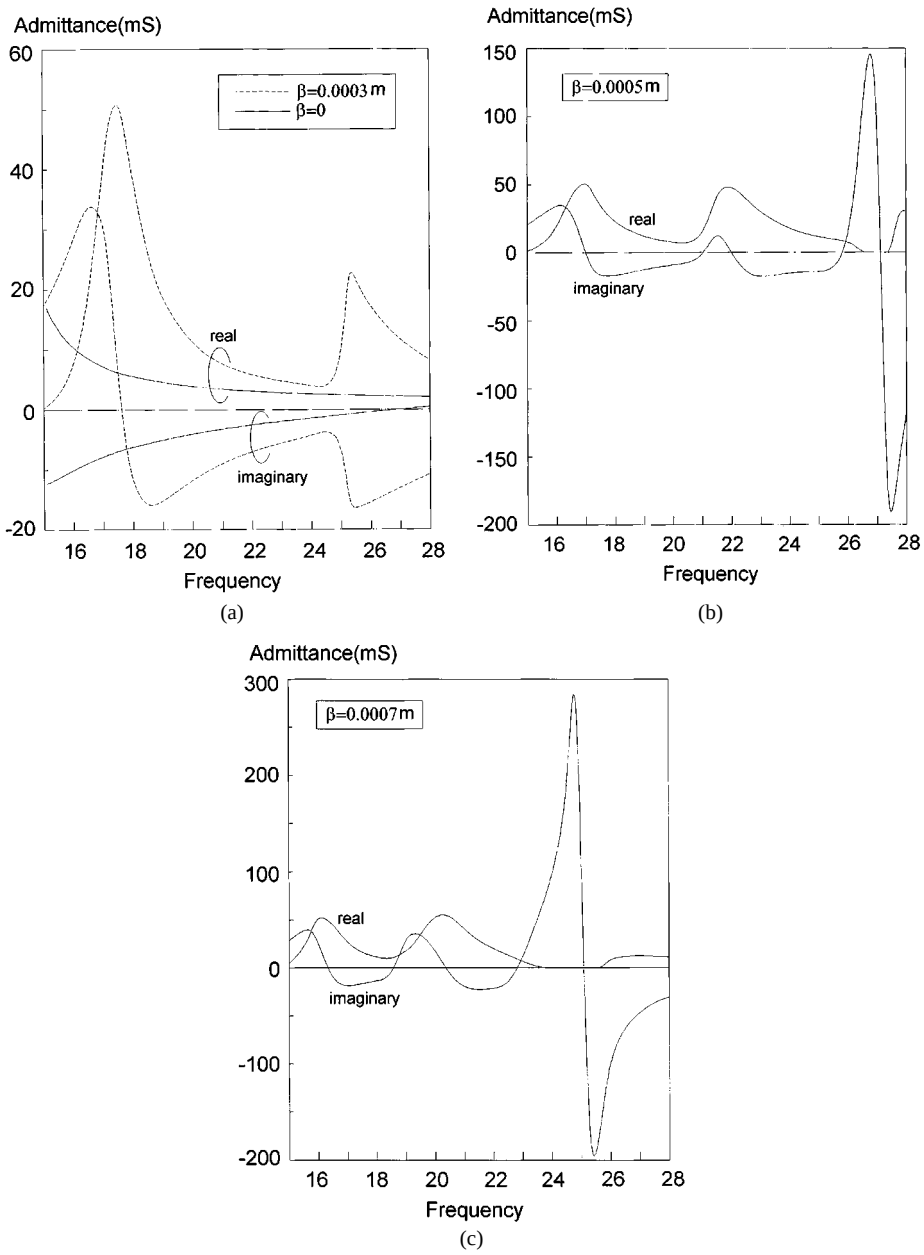

Fig. 4. Variations of the probe admittance with excitation frequency: (a) for $\beta = 0.0003$ m, (b) for $\beta = 0.0005$ m, and (c) for $\beta = 0.0007$ m.

waveguide, which are 27.5 GHz for $\beta = 0.0005$ m and 25.7 GHz for $\beta = 0.0007$ m.

The combined effect of these observations is that the admittance bandwidth shrinks in favor of a higher admittance level.

In Fig. 5, the variation of the probe admittance with the length of the coaxial probe (as a fraction of the waveguide separation d) is shown for $\beta = 0.0003$ m, $\beta = 0.0005$ m, and $\beta = 0.0007$ m, and for $d = 1$ cm, $a = 0.01$ cm, $b = 20a$, and $f = 22$ GHz, where f is the excitation frequency. We see that the chiral parameter has a significant effect on the resonant length of the coaxial probe (length at which the imaginary part of the admittance vanishes). All the three chiral cases give longer resonant probe lengths than the nonchiral one.

Finally, in Fig. 6, we show the computed current distributions along the coaxial probe for several chiral parameters and for $d = 1$ cm, $a = 0.01$ cm, $b = 20a$, $\ell = 0.5d$, and $f = 22$ GHz. It can be seen that, for all the chiral cases, the current magnitudes are greater than the nonchiral one, but all show a similar distribution.

V. Conclusions

The eigenfunction expansions of the complete set of four spatial-domain dyadic Green's functions for the parallel-plate chirowaveguide are derived rigorously and expressed in terms of the cylindrical vector wave functions. Using these dyadic Green's functions, both electric and magnetic fields due to arbitrarily distributed electric or magnetic or both current sources can be found. The coaxial-probe excitation method for the parallel-plate chirowaveguide is specifically analyzed by an EFIE formulated using the dyadic Green's functions. Solutions are obtained by the moment method. The probe input admittance

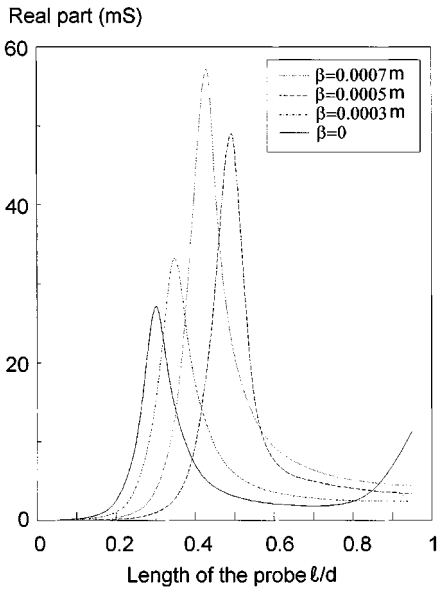

(a)

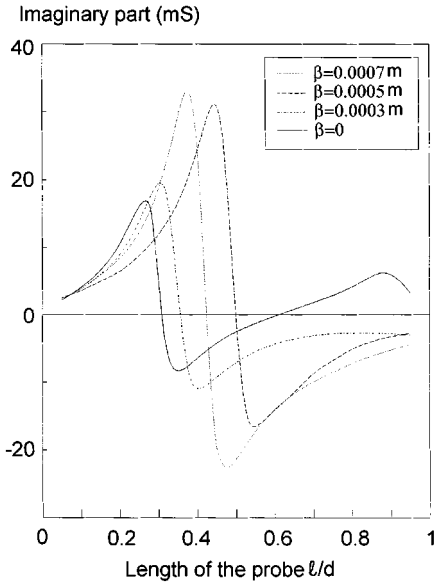

(b)

Fig. 5. Variation of the probe admittance with the length of the coaxial probe. (a) Real part. (b) Imaginary part.

and current distribution along the probe at different chiral levels are calculated. Results show that a substantially higher admittance level is obtained, but the admittance bandwidth decreases with an increasing chiral parameter. Stopbands at which no net power can be input into the waveguide are observed. These stopbands are found to be located near the cutoff frequencies. This new characteristic is found to have no match in the nonchiral waveguide. The computed current distribution along the probe shows that the current magnitude is greater than that of the nonchiral case.

APPENDIX

The expressions of two components of the dyadic Green's functions in the EFIE in (23) are presented in this section. As the electric current along the probe is considered

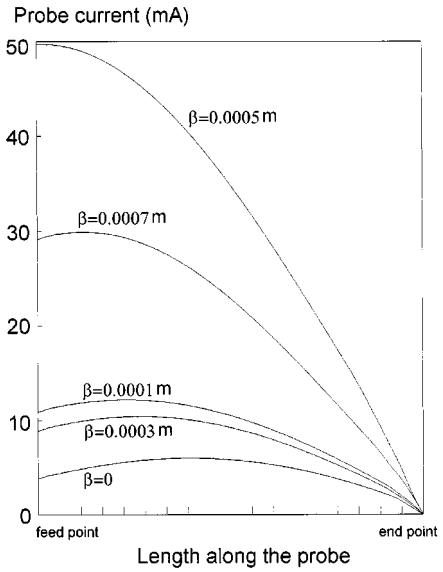

Fig. 6. Computed current distributions along the coaxial probe.

to be running along the central axis of the probe, we need only $[\overline{\overline{G}}^{+}_{EJ}(r, \phi, z; r', \phi', z')]_{\hat{z}\hat{z}}$, i.e., that part of $[\overline{\overline{G}}_{EJ}(r, \phi, z; r', \phi', z')]_{\hat{z}\hat{z}}$ for $r > r'$. From (20), it is given by

$$\begin{aligned}
&\left[\overline{\overline{G}}^{+}_{EJ}(r, \phi, z; r', \phi', z')\right]_{\hat{z}\hat{z}} \\
&= -\frac{1}{j\omega\mu}\sum_m\sum_n (\gamma/k)^2 H_n^{(1)}(\lambda_e r) J_n(\lambda_e r')\cos[n(\phi-\phi')] \\
&\quad\cdot\left\{\frac{\lambda_e^4}{I_e}\left\{\frac{(1+k\beta)}{k_1^2}\cos^2(k_{z2e}1/2\,d)\cos(k_{z1e}z)\cos(k_{z1e}z')\right.\right. \\
&\qquad+\frac{(1-k\beta)}{k_1k_2}\cos(k_{z2e}1/2\,d)\cos(k_{z1e}1/2\,d) \\
&\qquad\cdot\cos(k_{z1e}z)\cos(k_{z2e}z') \\
&\qquad+\frac{(1+k\beta)}{k_2k_1}\cos(k_{z1e}1/2\,d)\cos(k_{z2e}1/2\,d) \\
&\qquad\cdot\cos(k_{z2e}z)\cos(k_{z1e}z') \\
&\qquad+\frac{(1-k\beta)}{k_2^2}\cos^2(k_{z1e}1/2\,d)\cos(k_{z2e}z) \\
&\qquad\left.\cdot\cos(k_{z2e}z')\right\} \\
&\quad+\frac{\lambda_o^4}{I_o}\left\{\frac{(1+k\beta)}{k_1^2}\sin^2(k_{z2o}1/2d)\sin(k_{z1o}z)\sin(k_{z1o}z')\right. \\
&\qquad+\frac{(1-k\beta)}{k_1k_2}\sin(k_{z2o}1/2\,d)\sin(k_{z1o}1/2\,d) \\
&\qquad\cdot\sin(k_{z1o}z)\sin(k_{z2o}z') \\
&\qquad+\frac{(1+k\beta)}{k_2k_1}\sin(k_{z1o}1/2\,d)\sin(k_{z2o}1/2\,d) \\
&\qquad\cdot\sin(k_{z2o}z)\sin(k_{z1o}z') \\
&\qquad+\frac{(1-k\beta)}{k_2^2}\sin^2(k_{z1o}1/2\,d)\sin(k_{z2o}z) \\
&\qquad\left.\left.\cdot\sin(k_{z2o}z')\right\}\right\} \qquad \text{(A1)}
\end{aligned}$$

where $H_n^{(1)}$ is the Hankel function of the first kind and order n. The meanings of all other symbols are the same as those already discussed in Section II.

For computing the electric field due to the magnetic current $\vec{K}$ over the coaxial aperture, we need only $[\overline{\overline{G}}_{EK}(r, \phi, z; r', \phi', z')]_{\hat{z}\hat{\phi}}$ since $\vec{K}$ lies entirely outside the probe surface. From (11), the nonvanishing terms of $[\overline{\overline{G}}_{EK}(r, \phi, z; r', \phi', z')]_{\hat{z}\hat{\phi}}$ contributing to (23) are

$$\begin{aligned}
&\left[\overline{\overline{G}}_{EK}(r, \phi, z; r', \phi', z')\right]_{\hat{z}\hat{\phi}} \\
&= \frac{k}{j\omega\mu}\sum_m\sum_n(\gamma/k)^2 J_n(\lambda_e r)\frac{\partial H_n^{(1)}(\lambda_e r')}{\partial r'}\cos[n(\phi-\phi')] \\
&\quad\cdot\left\{\frac{\lambda_e^2}{I_e}\left\{\frac{(1+k\beta)}{k_1}\cos^2(k_{z2e}1/2\,d)\cos(k_{z1e}z)\cos(k_{z1e}z')\right.\right. \\
&\qquad+\frac{(1-k\beta)}{k_1}\cos(k_{z2e}1/2\,d)\cos(k_{z1e}1/2\,d) \\
&\qquad\cdot\cos(k_{z1e}z)\cos(k_{z2e}z') \\
&\qquad+\frac{(1+k\beta)}{k_2}\cos(k_{z1e}1/2\,d)\cos(k_{z2e}1/2\,d)\frac{1}{k_2} \\
&\qquad\cdot\cos(k_{z2e}z)\cos(k_{z1e}z') \\
&\qquad+\frac{(1-k\beta)}{k_2}\cos^2(k_{z1e}1/2\,d)\frac{1}{k_2}\cos(k_{z2e}z) \\
&\qquad\left.\cdot\cos(k_{z2e}z')\right\} \\
&\quad+\frac{\lambda_o^2}{I_o}\left\{\frac{(1+k\beta)}{k_1}\sin^2(k_{z2o}1/2\,d)\right. \\
&\qquad\cdot\sin(k_{z1o}z)\sin(k_{z1o}z') \\
&\qquad+\frac{(1-k\beta)}{k_1}\sin(k_{z2o}1/2\,d)\sin(k_{z1o}1/2\,d) \\
&\qquad\cdot\sin(k_{z1o}z)\sin(k_{z2o}z') \\
&\qquad+\frac{(1+k\beta)}{k_2}\sin(k_{z1o}1/2\,d)\sin(k_{z2o}1/2\,d) \\
&\qquad\cdot\sin(k_{z2o}z)\sin(k_{z1o}z') \\
&\qquad+\frac{(1-k\beta)}{k_2}\sin^2(k_{z1o}1/2\,d)\sin(k_{z2o}z) \\
&\qquad\left.\left.\cdot\sin(k_{z2o}z')\}\right\}. \qquad \text{(A2)}
\end{aligned}$$

We notice that by putting (A1) and (A2) into (23), we end up with two integrations and two infinite summations involved with $[\overline{\overline{G}}_{EJ}^{+}(r, \phi, z; r', \phi', z')]_{\hat{z}\hat{z}}$. (An additional integration is introduced by the matching procedure.) Fortunately, we find that the two integrations with respect to z and z' can be carried analytically, while the infinite summation with respect to n can be done by using the *addition theorem* for Hankel functions [18, pp. 232], which yields a single term. For $[\overline{\overline{G}}_{EK}(r, \phi, z; r', \phi', z')]_{\hat{z}\hat{\phi}}^{NM}$, we find that the integrations with respect to r' and ϕ' can be carried out analytically, yielding the following results:

$$\begin{aligned}
&\int_0^{2\pi}\int_a^b J_n(\lambda_e r)\frac{\partial H_n^{(1)}(\lambda_e r')}{\partial r'}\cos[n(\phi-\phi')]\frac{1}{r'}r'\,dr'\,d\phi' \\
&\quad=\begin{cases}2\pi J_0\left(\lambda_e a\right)\left[H_0^{(1)}\left(\lambda_e b\right)-H_0^{(1)}\left(\lambda_e a\right)\right], & n=0\\ 0, \qquad n\neq 0.\end{cases}
\end{aligned} \qquad \text{(A3)}$$

Thus, all the integrations and the infinite summation with respect to n vanish, leaving only the infinite summation with respect to m. This allows very efficient numerical codes to be written.

REFERENCES

[1] S. Bassiri, N. Engheta, and C. H. Papas, "Dyadic Green's function and dipole radiation in chiral media," *Alta Freq.*, vol. 55, pp. 83–88, 1986.

[2] I. V. Lindell, A. H. Sihvola, S. A. Tretyakov, and A. J. Viitanen, *Electromagnetic Waves in Chiral and Bi-Isotropic Media*. Norwood, MA: Artech House, 1994.

[3] N. Engheta and M. W. Kowarz, "Antenna radiation in the presence of a chiral sphere," *J. Appl. Phys.*, vol. 67, no. 2, pp. 639–647, 1990.

[4] A. Toscano and L. Vegni, "Spectral dyadic Green's function formulation for planar integrated structures with a grounded chiral slab," *J. Electromag. Waves Applicat.*, vol. 6, pp. 751–769, 1992.

[5] S. M. Ali, T. M. Habashy, and J. A. Kong, "Spectral-domain dyadic Green's function in layered chiral media," *J. Opt. Soc. Amer. A, Opt. Image Sci.*, vol. 9, pp. 413–423, 1992.

[6] L. W. Li, P. S. Kooi, M. S. Leong, and T. S. Yeo, "A general expression of dyadic Green's functions in radially multilayered chiral media," *IEEE Trans. Antennas Propagat.*, vol. 43, pp. 232–238, Feb. 1995.

[7] H. T. Hui and E. K. N. Yung, "The eigenfunction expansion of dyadic Green's functions for chirowaveguides," *IEEE Trans. Microwave Theory Tech.*, vol. 44, pp. 1575–1583, Sept. 1996.

[8] ——, "Corrections to 'The eigenfunction expansion of dyadic Green's functions for chirowaveguides'," *IEEE Trans. Microwave Theory Tech.*, vol. 45, p. 561, Apr. 1997.

[9] ——, "The eigenfunction expansion of dyadic Green's functions for the parallel-plate chirowaveguides," *Proc. Inst. Elect. Eng.*, vol. 145, pp. 273–278, 1998.

[10] E. L. Tan and S. Y. Tan, "Dyadic Green's functions for circular waveguides filled with biisotropic media," *IEEE Trans. Microwave Theory Tech.*, vol. 47, pp. 1134–1137, July 1999.

[11] B. R. Rao, "Current distribution and impedance of an antenna in a parallel-plate region," *Proc. Inst. Elect. Eng.*, vol. 112, pp. 259–268, 1965.

[12] D. V. Otto, "The admittance of cylindrical antennas driven from a coaxial line," *Radio Sci.*, vol. 2, pp. 1031–1042, 1967.

[13] Z. Shen and R. H. MacPhie, "Modal expansion analysis of monopole antennas driven from a coaxial line," *Radio Sci.*, vol. 31, pp. 1037–1046, 1996.

[14] D. L. Jaggard, J. C. Liu, A. Grot, and P. Pelet, "Radiation and scattering from thin wires in chiral media," *IEEE Trans. Antennas Propagat.*, vol. 40, pp. 1273–1282, Nov. 1992.

[15] A. Lakhtakia, *Beltrami Fields in Chiral Media*. Singapore: World Scientific, 1994.

[16] C. T. Tai, *Dyadic Green Functions in Electromagnetic Theory*. Piscataway, NJ: IEEE Press, 1994.

[17] N. Engheta and P. Pelet, "Modes in chirowaveguides," *Opt. Lett.*, vol. 14, pp. 593–595, June 1989.

[18] R. F. Harrington, *Time-Harmonic Electromagnetic Fields*. New York: McGraw-Hill, 1961.

Hon-Tat Hui (S'94–A'98–M'00) was born in China and emigrated to Hong Kong in 1978. He received the B.Eng. degree (with first-class honors) in electronic engineering and the Ph.D. degree from the City University of Hong Kong, Kowloon, Hong Kong, in 1994 and 1998, respectively.

Since 1998, he has been a Research Fellow in the Wireless Communication Center, City University of Hong Kong. His current research interests include method of moments (MoM) computational aspects for complex media, computations of dyadic Green's functions, computational electromagnetics of thin-wire scatterers and antennas, computations of microstrip structures, and the analysis and design of small antennas for mobile communications.

Edward K. N. Yung (M'85–SM'85) received the B.S., M.S., and Ph.D. from the University of Mississippi, University, in 1972, 1974, and 1977, respectively.

In 1984, he joined the City University of Hong Kong, Kowloon, Hong Kong. In 1989, he became a Full Professor and, in 1994, was awarded a personal chair. He is the Founding Director of the Wireless Communications Research Center, City University of Hong Kong, where he is currently the Head of the Electronic Engineering Department. He is also the Principle Investigator of many research projects. He has authored or co-authored over 100 papers and holds one patent. He is listed in *Who's Who in the World* and *Who's Who in the Science and Engineering in the World*.

Dr. Yung is a Fellow of the Chinese Institution of Electronics and the Hong Kong Institution of Engineers (HKIE). He is a member of Eta Kappa Nu, Phi Kappa Phi, Tau Beta Pi, and the Electromagnetics Academy.

Xin-Qing Sheng was born in Anhui, China, in 1968. He received the B.S., M.S., and Ph.D. degrees from the University of Science and Technology of China (USTC), Hefei, China, in 1991, 1994, and 1996, respectively.

From 1994 to 1996, he was a Research Assistant in the Department of Electronic Engineering and Information Science, USTC, where he developed a code of hybridization of the finite-element method and mode-matching method for discontinuity problems in waveguides. From 1996 to 1998, he was with the Center for Computational Electromagnetics, Department of Electrical and Computer Engineering, University of Illinois at Urbana-Champaign, where he developed a code of the MLFMA-enhanced finite-element boundary-integral method for large coated bodies. Since 1998, he has been a Research Fellow with the City University of Hong Kong, Kowloon, Hong Kong, where he is currently supervising several projects. His research interests focus on computational electromagnetics covering computer solutions of scattering, radiation, and transmission problems, computing algorithms, and application of achievement in mathematics and computer science.